Laser triggered Z-pinch broadband extreme ultraviolet source for metrology

I. Tobin, L. Juschkin, Y. Sidelnikov, F. O'Reilly, P. Sheridan et al.

Citation: Appl. Phys. Lett. **102**, 203504 (2013); doi: 10.1063/1.4807172
View online: http://dx.doi.org/10.1063/1.4807172
View Table of Contents: http://apl.aip.org/resource/1/APPLAB/v102/i20
Published by the American Institute of Physics.

Laser triggered Z-pinch broadband extreme ultraviolet source for metrology

I. Tobin,[1] L. Juschkin,[2,3] Y. Sidelnikov,[4] F. O'Reilly,[2] P. Sheridan,[5] E. Sokell,[2] and J. G. Lunney[1,a)]
[1]*School of Physics, Trinity College Dublin, Dublin 2, Ireland*
[2]*School of Physics, University College Dublin, Belfield, Dublin 4, Ireland*
[3]*Department of Physics, RWTH Aachen University, Steinbachstr. 15 D-52074 Aachen, Germany*
[4]*ISAN Institute of Spectroscopy, Fizicheskaya Str. 5, Troitsk, Moscow Region 142190, Russia*
[5]*Newlambda Technologies, UCD Science Centre North, Belfield, Dublin 4, Ireland*

(Received 20 December 2012; accepted 4 May 2013; published online 21 May 2013)

We compare the extreme ultraviolet emission characteristics of tin and galinstan (atomic %: Ga: 78.35, In: 14.93, Sn: 6.72) between 10 nm and 18 nm in a laser-triggered discharge between liquid metal-coated electrodes. Over this wavelength range, the energy conversion efficiency for galinstan is approximately half that of tin, but the spectrum is less strongly peaked in the 13–15 nm region. The extreme ultraviolet source dimensions were 110 ± 25 μm diameter and 500 ± 125 μm length. The flatter spectrum, and -19 °C melting point, makes this galinstan discharge a relatively simple high radiance extreme ultraviolet light source for metrology and scientific applications. [http://dx.doi.org/10.1063/1.4807172]

Laser produced plasmas (LPPs) and discharge produced plasmas (DPPs) have been extensively studied as radiation sources for extreme ultraviolet (EUV) lithography at 13.5 nm.[1] Current state-of-the-art sources use tin as the emitter material because it has strong emission at 13.5 nm due to 4 p–4 d and 4 d–4f unresolved transition arrays (UTAs) in Sn XI–XIV.[2] Discharge sources have the potential to provide higher wall-plug efficiency than LPPs.[3] EUV emission from a Z-pinch in a laser-triggered discharge between rotating electrodes coated with liquid tin has been studied previously.[4,5] The liquid metal coating overcomes the problem of electrode erosion, but it is necessary to maintain the tin above its melting temperature of 232 °C. The EUV emission spectrum of pure tin plasma, at the appropriate conditions, is relatively narrow-band, with ~50% of emission in the 13–15 nm range. For EUV metrology, the source parameters of interest are spectral radiance, wavelength range, and emission uniformity, as well as cost and ease of operation. Compared to pure tin, galinstan (at. %: Ga: 78.35, In: 14.93, Sn: 6.72) has spectrally flat broadband emission in the 10–18 nm range arising from each of its transition-rich constituents. This makes galinstan a useful source for reflectrometry, where the reflectivity of EUV mirrors needs to be measured over an extended wavelength range for the detection of reflectance inhomogeneities. Being liquid at room temperature makes a galinstan-based source somewhat simpler in construction and operation than those using higher melting point materials. Like tin, galinstan can also be utilized as a mirror coating in collector optics,[6] thus avoiding damage of the EUV collector by plasma deposition or ion sputtering. This paper describes the results of an experiment to characterise the EUV emission of laser-triggered Z-pinch discharges in galinstan, which has not been studied before in this type of source. The spatial and spectral characteristics of the EUV emission, along with ion outflow, are investigated for different discharge energies. Comparison is made with laser triggered discharges in tin which are similar to the state-of-the-art sources for 13.5 nm lithography.

The Z-pinch EUV source is based on a laser-triggered discharge struck between two rotating disc electrodes, which are coated in liquid metal by partial immersion in liquid metal baths. The source was developed at the Russian Institute of Spectroscopy (ISAN).[5] Figure 1 shows plan and side views of the electrode geometry and the arrangement of the diagnostic instruments. The disc electrodes are tilted so that the separation at closest approach is 4 mm. For galinstan, the metal baths are not heated, while for tin they are heated to 300 °C. The anode is grounded to the chamber while the cathode is connected to the live electrode of a 0.39 μF capacitor bank. The charging voltage was varied from 2.5 to 5.5 kV (1.25 to 6.05 J).

The discharge is triggered using a 1064 nm, 30 ns laser pulse to form a LPP on the cathode electrode at the point of closest approach to the anode. The laser is focused to a 400 μm diameter spot and the energy was varied in the range of 5–80 mJ by means of a rotatable half-wave plate and polarizing beam splitter. The laser operates at a maximum repetition rate of 2 Hz or in single pulse mode. The LPP expands away from the cathode and triggers the discharge when it reaches the anode. The derivative of the discharge current is recorded using a Rogowski coil placed in the vicinity of the current path between the capacitor and the cathode.

A 0.057 cm^2 aperture Faraday cup ion detector, placed in the horizontal plane at a distance of 50 cm from the discharge and at an angle of 60° from the discharge axis (facing cathode), was used to monitor the plasma outflow from the discharge. The cup collector was biased at -12 V to reject plasma electrons and was equipped with a 65 mT transverse magnetic field to suppress the detection of ion-induced secondary electron emission and photo-electron emission due to vacuum ultraviolet and EUV emission from the plasma. From the ion time-of-flight (TOF) measurements recorded with the cup, it is possible to estimate the ion energy distribution and ion flux at the position of the cup. These values are of interest for assessing the level of ion sputtering of any

a)Author to whom correspondence should be addressed. Electronic mail: jlunney@tcd.ie

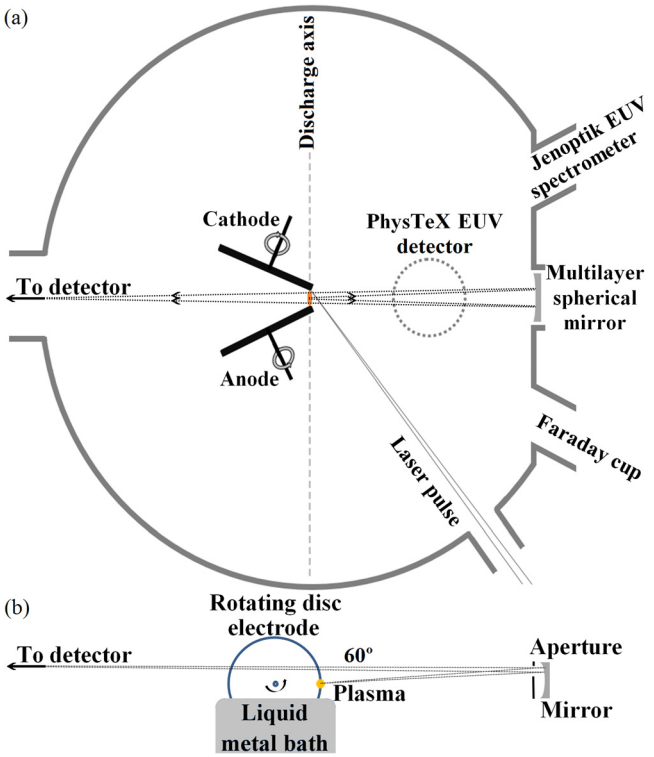

FIG. 1. Schematic (a) plan and (b) side-view of laser triggered Z-pinch discharge EUV source and the diagnostic instruments.

optical element placed near the discharge, or for the design of systems to mitigate such sputtering.

Several devices were used to measure the EUV emission. The time-integrated emission spectrum was measured in the 10–18 nm range using an absolutely calibrated grazing incidence Jenoptik spectrometer equipped with a back illuminated silicon CCD detector[7,8] viewing the plasma in the horizontal plane at 60° from the discharge axis facing the anode. The spectral resolution of the spectrometer is ~0.03 nm. The absolute emission in a 2% bandwidth at 13.5 nm was measured with a PhysTeX EUV detector comprised of a calibrated EUV sensitive photodiode[9,10] combined with two Mo/Si multilayer mirrors and a 250 nm thick Zr filter. The PhysTeX EUV detector viewed the plasma at 60° above the horizontal plane but normal to the discharge axis. Thus, it was possible to make two independent measurements of the EUV emission at different angles with respect to the discharge axis. The spatial distribution of the EUV source was recorded by using a 125 mm radius spherical Mo/Si multilayer mirror at near normal incidence to form a 13× magnified image on a CCD, as shown in Fig.1. The imaging system had a resolution of ~5 μm and included a 1 μm Zr filter to provide spectral filtering in the 10–18 nm region.

Figure 2 shows the derivative of the discharge current, recorded using the Rogowski coil, and the discharge current obtained by integration, for a 4 J galinstan discharge triggered using a 5 mJ laser pulse. The weakly damped discharge, which has a period of ~660 ns, was modelled over the first two periods to yield a value of 25 nH for the overall inductance and 60 mΩ for the average plasma resistance. It can be seen that the discharge current begins to rise at ~300 ns after the laser pulse, which is associated with the transit time of the LPP across the 4 mm inter-electrode gap.

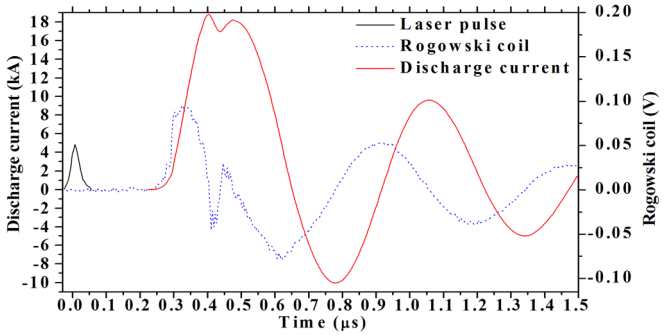

FIG. 2. Derivative of the discharge current as recorded by the Rogowski coil (dashed line) and the discharge current (solid line) obtained by integration for a galinstan discharge triggered by a 5 mJ laser pulse with a charging voltage of 4.5 kV (4 J).

The delay between the laser pulse and the onset of the discharge depends on both the laser energy and the charging voltage. It was noted that the discharge in tin has a somewhat shorter period at ~620 ns, with the discharge current beginning at ~150 ns after the laser pulse; in that case the laser energy was 12 mJ, which will produce a more energetic ablation plume expansion. A short duration disruption of the damped sinusoid is observed at ~420 ns, which is associated with the rapid rise of the plasma impedance caused by Z-pinching of the plasma column; the presence of this feature indicates that Z-pinching has occurred. The timing of the pinch can be adjusted relative to the discharge by varying the energy of the laser pulse so that the pinch occurs when the current reaches its first maximum, which was observed to be optimum for the EUV output. The laser energy was 5 mJ for galinstan and 12 mJ for tin for all the results presented here. Under these trigger conditions, it was found that at 5.5 kV the fraction of discharges leading to a pinch was ~75% for galinstan and ~90% for tin.

The EUV imaging system, described above, has a ~1.3 mm diameter moveable field of view and a spatial resolution of ~5 μm. Figure 3 shows a time-integrated EUV image of a typical galinstan discharge where pinching occurs. The image has been processed to remove the contribution due to illumination from the plasma that had not reached the detector via the imaging mirror, and the shadow cast by the filter mesh. Since Z-pinch discharges are intrinsically unstable, there is some shot-to-shot variation in the location and shape of the EUV emitting region. By measuring the full widths at half maximum, the cylindrically shaped galinstan EUV source was found to have an average diameter of 110 μm ± 25 μm and length of 500 μm ± 125 μm.

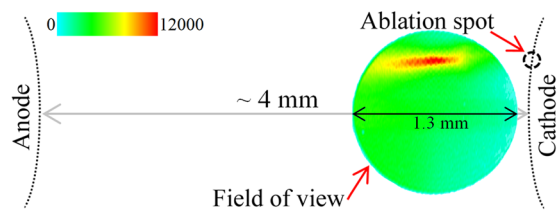

FIG. 3. Time-integrated EUV emission of a typical 4.05 J discharge in galinstan triggered by a 5 mJ, 30 ns laser pulse. The schematic shows that the 1.3 mm diameter field of view is located in the 4 mm inter-electrode gap, but closer to cathode.

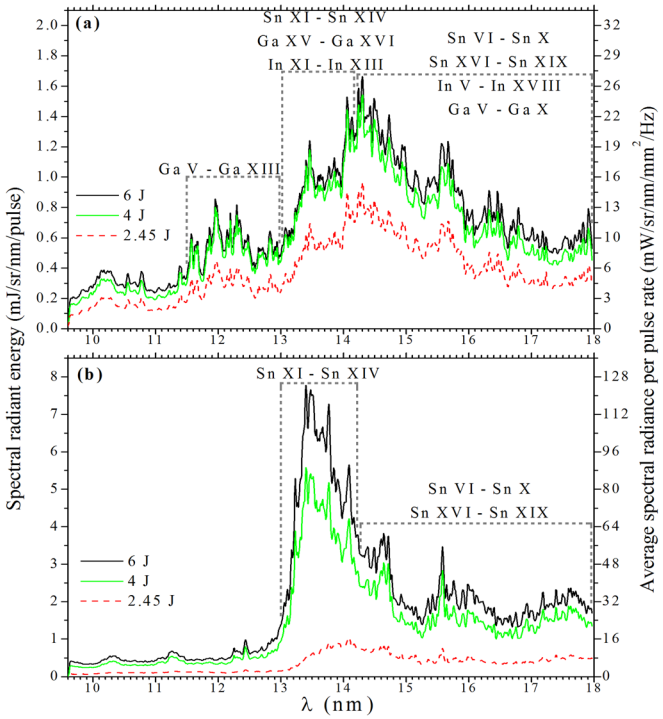

FIG. 4. Spectral radiant energy and average spectral radiance per pulse rate emitted from pinching discharges in (a) galinstan and (b) tin for different discharge energies. The ion stages contributing to the emission in different spectral regions are indicated.

Figure 4 shows the EUV spectral radiant energy, and average spectral radiance per pulse rate, of galinstan and tin for a range of discharge energies, as measured with the grazing incidence spectrometer. The tin spectra provide a useful benchmark for the EUV performance of the galinstan plasmas, under the same range of conditions. The tin spectra show the expected UTA in the range of 13–15 nm as has been reported for both discharge[3–5,11] and LPP[12,13] sources. For galinstan, the tin UTA is also observed, but transitions in the range of 11.5–13 nm, due to gallium, and 14–18 nm, due to both gallium and indium, are also present. According to calculations with the Cowan code,[14] for both indium and tin the strongest emission is due to 4 p-4 d and 4 d-4f transitions, while for gallium it is due to 3 p-3 d, 3 d-4 p, and 3 d-4f transitions.[15]

Figure 4 shows the spectral distribution of the EUV from the galinstan source is relatively insensitive to the discharge energy. Thus, the emission in a 2% band at 13.5 nm, which is widely used to characterise EUV emission from tin plasmas, is a useful proxy for the emission across the broader spectral range of relevance to metrology applications. Figure 5 shows how the EUV emission energy in the 2% band, as measured with the absolutely calibrated PhysTeX EUV detector, depends on the discharge energy for both tin and galinstan plasmas. For both cases, the EUV emission increases with discharge energy. For tin, the in-band EUV output increases quite sharply as the discharge energy is raised from 3 J to 4 J and then more slowly up to 6 J, while for galinstan, the in-band radiation grows more steadily over the range of discharge energies investigated. The discharge energy dependence of the galinstan in-band emission as measured with the PhysTeX detector, and Jenoptik spectrometer, are similar, though the viewing angles are different, as described above.

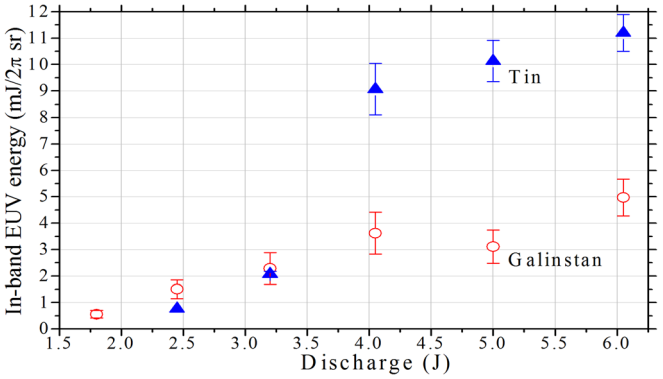

FIG. 5. Discharge energy dependence of the in-band (2% bandwidth centered at 13.5 nm) EUV emission into 2π sr measured with the PhysTeX detector for tin (▲) and galinstan (○).

In the design of an EUV source for metrology, it is necessary to characterise, and perhaps mitigate, the ionic, neutral, and particulate material impinging on the first EUV optical element. The Faraday cup was used to record the ion flux associated with the plasma outflow; typical ion signals for 4 J discharges in galinstan and tin are shown in Fig. 6. These are obtained by averaging over 32 consecutive discharges. While a Faraday cup does not give any information about the ion charge distribution, if an average value of ion charge is assumed, then the ion TOF signal can be used to determine the energy distribution and fluence of ions at the position of the Faraday cup. For tin with an estimated average ion charge of ~12, the peak of the TOF signal corresponds to 2.4 keV, the average ion energy is ~2.2 keV, and the total ion fluence per discharge at 50 cm is 4.3×10^{10} ions cm^{-2}. For galinstan, gallium is the primary constituent and the average ion charge is expected to be ~10, and the corresponding values are 4.6 keV, 2.4 keV, and 3.8×10^{10} ions cm^{-2}. Due to differing experimental arrangements and reporting conventions, direct comparison of ion fluence is sometimes difficult, but it can be noted that the ion energies observed here are of the same order as those for LPPs from tin targets.[16]

In summary, the spatial and spectral characteristics of the EUV emission from laser-triggered Z-pinch galinstan plasmas have been measured and compared with the emission from tin plasmas, which have been widely studied as sources for EUV lithography. Whilst galinstan plasmas have

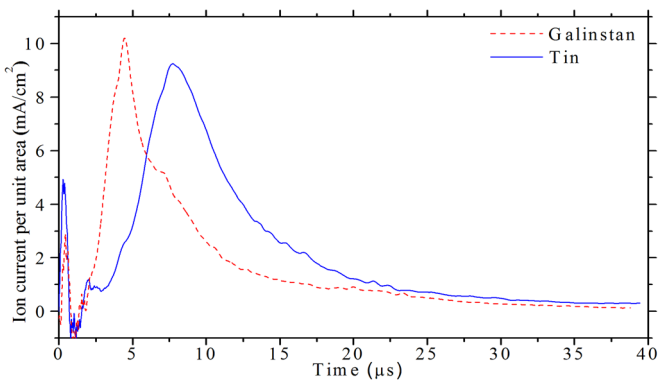

FIG. 6. Faraday cup ion time-of-fight signals for 4 J discharges, in tin (—) and galinstan (---).

lower in-band conversion efficiencies than tin plasmas, the EUV emission from galinstan has a broader, less sharply peaked spectral profile, due to the emission from the indium and gallium constituents. Thus, a galinstan source is more suited to EUV metrology applications like reflectrometry of EUV optics and mask blanks. Furthermore, the use of galinstan allows continuously rotating liquid-metal coated electrodes, which are required for high repetition rate, to be provided at room temperature, which simplifies the design and operation of small laboratory, or metrology, EUV sources. For both galinstan and tin, the EUV output increases strongly when the plasma is Z-pinched. Pinching occurs most readily when the energy in the laser ablation pulse is adjusted so that the pinch occurs at the time of the first maximum of the discharge current. Future studies to optimise the stability and reproducibility of the EUV emission from laser-triggered Z-pinch galinstan-based plasmas will pave the way for development of laboratory-based metrology sources that may be used over a range of EUV wavelengths.

This publication resulted from research conducted with the financial support of Science Foundation Ireland under grant "SFI 07/IN.1/I1771," by Enterprise Ireland under grants "TD20090346" and "PC/07/069" and co-funded by the European Regional Development fund. This research was supported by the technical staff in the mechanical and electronics workshops in University College Dublin. The authors also acknowledge Imam Kambali for the theoretical calculations of gallium, indium, and tin transitions using Cowan code.

[1]V. Bakshi, *EUV Lithography* (SPIE Press, Bellingham, WA, 2006).
[2]G. O'Sullivan and R. Faulkner, Opt. Eng. **33**(12), 3978 (1994).
[3]G. Schriever, O. Semprez, J. Jonkers, M. Yoshioka, and R. Apetz, J. Micro/Nanolith. MEMS MOEMS **11**(2), 021104 (2012).
[4]K. Gielissen, Y. Sidelnikov, D. Glushkov, W. A. Soer, V. Banine, and J. J. A. M. V. D. Mullen, J. Appl. Phys. **107**, 013301 (2010).
[5]V. Y. Banine, K. N. Koshelev, and G. H. P. M. Swinkels, J. Phys. D **44**, 253001 (2011).
[6]K. Fahy, F. O'Reilly, E. Scally, and P. Sheridan, Proc. SPIE **7802**, 78020K (2010).
[7]M. C. Schuermann, T. Missalla, K. R. Mann, S. Kranzusch, R. M. Klein, F. Scholze, G. Ulm, R. Lebert, and L. Juschkin, Proc. SPIE **5037**, 378 (2003).
[8]T. Missalla, M. C. Schuermann, R. Lebert, C. Wies, L. Juschkin, Roman M. Klein, F. Scholze, G. Ulm, A. Egbert, B. Tkachenko, and B. N. Chichkov, Proc. SPIE **5374**, 979 (2004).
[9]L. A. Shmaenok, in International SEMATECH EUV Source Workshop Meeting, February 2004.
[10]P. Dunne, O. Morris, E. Sokell, F. O'Reilly, G. O'Sullivan, N. Murphy, P. Hayden, and V. Bakshi, SEMATECH Document ID No. 06114813A-ENG (2006).
[11]M. Yoshioka, Y. Teramoto, J. Jonkers, M. C. Schürmann, R. Apetz, V. Kilian, and M. Corthout, Proc. SPIE **7969**, 79691G (2011).
[12]P. Hayden, A. Cummings, N. Murphy, G. O'Sullivan, P. Sheridan, J. White, and P. Dunne, J. Appl. Phys. **99**, 093302 (2006).
[13]J. White, P. Dunne, P. Hayden, F. O'Reilly, and G. O'Sullivan, Appl. Phys. Lett. **90**, 181502 (2007).
[14]R. D. Cowan, *Theory of Atomic Structure and Spectra* (University of California Press, Berkeley, CA, 1981).
[15]I. Kambali, private communication (2012).
[16]R. W. Coons, S. S. Harilal, D. Campos, and A. Hassanein, J. Appl. Phys. **108**, 063306 (2010).